Macrocyclic Inhibitors of Penicillopepsin. 2. X-ray Crystallographic Analyses of Penicillopepsin Complexed with a P3−P1 Macrocyclic Peptidyl Inhibitor and with Its Two Acyclic Analogues

Jinhui Ding,[†] Marie E. Fraser,[†] J. Hoyt Meyer,[‡] Paul A. Bartlett,[‡] and Michael N. G. James*,[†]

Contribution from the Medical Research Council of Canada Group in Protein Structure and Function, Department of Biochemistry, University of Alberta, Edmonton, Alberta, Canada T6G 2H7, and Department of Chemistry, University of California, Berkeley, California 94720-1460

Received October 27, 1997

Abstract: Macrocyclic inhibitor **1** {methyl [cyclo-7[(2*R*)-((*N*-valyl) amino)-2-(hydroxyl-(1*S*)-1-methyoxycarbonyl-2-phenylethoxy)phosphinyloxyethyl]-1-naphthaleneacetamide] sodium salt} was designed according to the conformation of the acyclic analogue Iva-L-Val-L-Val-L-Leu^{P}-(O)Phe-OMe [Leu^{P} = the phosphinic acid and analogue of L-leucine; (O)Phe = L-3-phenyllactic acid; OMe = methyl ester] (**4**) bound to penicillopepsin, by linking the P1 and P3 side chains of the penicillopepsin inhibitor. This compound and its two acyclic derivatives, {methyl (2*S*)-[1-(((*N*-Formyl)-L-valyl)amino-2-(2-naphthyl)ethyl)hydroxyphosphinyloxy]-3-phenylpropanoate, sodium salt} (**2**) and {methyl (2*S*)-[1-(((*N*-(1-naphthaleneacetyl))-L-valyl)aminomethyl)hydroxyphosphinyloxy]-3-phenylpropanoate, sodium salt} (**3**), have been synthesized and evaluated as inhibitors of penicillopepsin. Their binding affinity to the enzyme was found to be inversely related to the predicted degree of conformational flexibility across the series: **3** (K_i = 110 μM), **2** (K_i = 7.6 μM), **1** (K_i = 0.8 μM). The X-ray crystallographic structures of penicillopepsin complexed with the macrocyclic peptidyl phosphonate **1** and with its two derivatives **2** and **3** have been determined and refined to crystallographic agreement factors R ($=\Sigma||F_o| - |F_c||/\Sigma|F_o|$) of 15.9%, 16.0%, and 15.2% and R_{free} of 19.8%, 20.3%, and 21.4%, respectively. The intensity data for all complexes were collected to 1.5 Å resolution. One 1.25 Å resolution data set was obtained for the complex with **1** at 110 K; the structure was refined to an R factor of 15.0% (R_{free} of 19.7%). The binding interactions that **1** and **2** make with penicillopepsin are similar to those that have been observed for other transition-state mimics with aspartyl proteinases. On the other hand, the acyclic linear inhibitor **3** exhibits distinctive binding to penicillopepsin with the phosphonate group shifted ~3.0 Å from the average position observed for the other complexes. These structural results show that the macrocyclic constraint of **1** enhances its binding affinity over those of the acyclic analogues but the differences in the observed bound dispositions mean that the effect has yet to be quantified.

Introduction

Penicillopepsin (EC 3.4.23.X) is an aspartyl proteinase isolated from the mold *Penicillium janthinellum*. It contains 323 amino acids in its single polypeptide chain. This fungal enzyme is homologous to the mammalian enzyme pepsin.[1] The crystal structure analyses of a variety of aspartyl proteinases have shown that they consist of two major similarly-folded, predominantly β-sheet domains, the junction of which forms an extended binding cleft for oligopeptide substrates. The two catalytic aspartyl residues of these enzymes, located one on each domain, extend their side-chain carboxyl groups to the cleft center.[2−4] In penicillopepsin, the two aspartyl residues at the active site are Asp213 acting as a general base and Asp33 as a general acid; a central nucleophilic water molecule is bound between the two carboxyl groups.[5]

It is known that various phosphorus-containing peptides are potent inhibitors of the aspartyl proteinases.[6−9] A series of phosphonate tetrapeptides have been shown to be transition-state analogues for pepsin.[8] Studies on crystal structures of aspartyl proteinases complexed with phosphonate tetrapeptides provide a solid structural basis to characterize these compounds as transition-state mimics. The X-ray crystal structures of complexes between fungal penicillopepsin and three tetrahedral phosphinate and phosphonate inhibitors, including Iva-L-Val-L-Val-L-Leu^{P}-(O)Phe-OMe [Leu^{P} = the phosphoric acid ana-

* Author to whom correspondence should be addressed: tel (403) 492-4550; fax (403) 492-0886; email michael.james@ualberta.ca.
[†] University of Alberta.
[‡] University of California.

(1) Sodek, J.; Hofmann, T. *Can. J. Biochem.* **1970**, *48*, 1014−1016.
(2) Hsu, I.-N.; Delbaere, L. T. J.; James, M. N. G. *Nature* **1977**, *266*, 140−145.
(3) Subramanian, E.; Swan, I. D. A.; Liu, M.; Davies, D. R.; Jenkins, J. A.; Tickle, I. J.; Blundell, T. L. *Proc. Natl. Acad. Sci. U.S.A.* **1977**, *74*, 556−559.
(4) Tang, J.; James, M. N. G.; Hsu, I. N.; Jenkins, J. A.; Blundell, T. L. *Nature* **1978**, *271*, 618−621.
(5) James, M. N. G.; Sielecki, A. R.; Hayakawa, K.; Gelb, M. H. *Biochemistry* **1992**, *31*, 3872−3886.
(6) Bartlett, P. A.; Hanson, J. E.; Giannousis, P. P. *J. Org. Chem.* **1990**, *55*, 6268−6274.
(7) Abdel-Meguid, S. S.; Zhao, B.; Murthy, K. H. M.; Winborne, E.; Choi, J.-K.; DesJarlais, R. L.; Minnich, M. D.; Culp, J. S.; Debouck, C.; Tomaszek, T. A., Jr.; Meek, T. D.; Dreyer, G. B. *Biochemistry* **1993**, *32*, 7972−7980.
(8) Bartlett, P. A.; Giangiordano M. A. *J. Org. Chem.* **1996**, *61*, 3433−3438.
(9) Meyer, J. H.; Bartlett, P. A. *J. Am. Chem. Soc.* **1998**, *120*, 4600

S0002-7863(97)03714-1 CCC: $15.00
Published on Web 05/05/1998

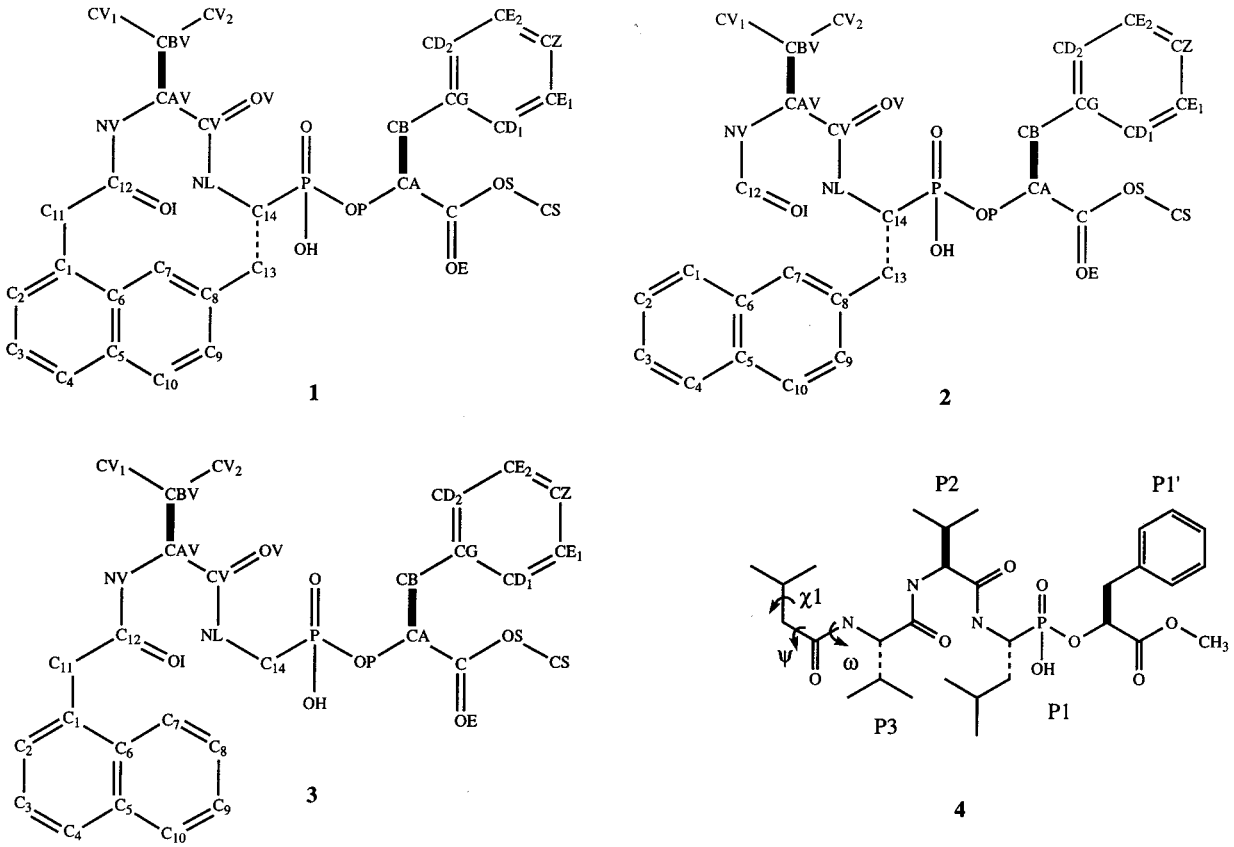

Figure 1. Diagrams of **1**−**4**. The atom labeling is that used in the body of the paper.

logue of L-leucine; (O)Phe = L-3-phenyllactic acid; OMe = methyl ester] (**4**), were determined.[10] All three inhibitors bound identically in the active site at the catalytic aspartyl residues of this enzyme, in imitation of the transition state for substrate hydrolysis. This work also showed that the *pro-S* oxygen atom of the two phosphonate inhibitors and of the phosphinate group of the Sta(P) inhibitor make very short contact distances (approximately 2.4 Å) to the carboxyl oxygen atom, Oδ1, of Asp33 on penicillopepsin. This distance and the stereochemical environment of the carboxyl and phosphonate groups were interpreted in terms of a hydrogen bond that most probably has a symmetric single-well potential energy function. Subsequently, similar characteristics were reported in a crystallographic analysis of a complex between the human immunodeficiency virus type 1 (HIV-1) proteinase and its competitive inhibitor, a C_2-symmetric phosphinate.[7] This working model of the aspartyl proteinases complexed with transition-state analogues has recently received more support from crystal structure analyses such as those of pepsin,[11] rhizopuspepsin,[12] and endothiapepsin[13] and from Fourier transform infrared spectroscopic studies.[14,15] In addition, an energetic analysis for such a catalytic pathway suggested that electronic effects are mainly responsible for the relative reduction of energy of the intermediates and possibly transition states on the catalytic reaction path.[16]

According to the conformation of the acyclic peptidyl inhibitor, Iva-L-Val-L-Val-L-Leu(P)-(O)Phe-OMe bound to penicillopepsin,[10] a macrocyclic peptidyl phosphonate {methyl[cyclo-7[(2*R*)-((*N*-valyl)amino)-2-(hydroxyl-(1*S*)-1-methyloxycarbonyl-2-phenylethoxy)phosphinyloxyethyl]-1-naphthaleneacetamide] sodium salt} (**1**) was designed linking the P1 and P3 side chains of the penicillopepsin inhibitor.[9] This compound and its two acyclic derivatives **2** and **3** (Figure 1) have been synthesized and evaluated as inhibitors of penicillopepsin.[9]

The two acyclic compounds **2** and **3** were designed to distinguish the effect of macrocyclization from that of the hydrophobic binding energy. The binding affinities of these compounds for penicillopepsin were found to be inversely related to the degree of conformational flexibility across the series: **3** (K_i = 110 μM), **2** (K_i = 7.6 μM), **1** (K_i = 0.8 μM). In addition, the NMR analyses combined with molecular modeling suggested that **1** could fit in the penicillopepsin active site with a movement of the aromatic naphthalene linker away from one wall of the binding pocket.[9] To firmly characterize the effects of linking the side chains of these phosphonate tetrapeptides on the binding to the fungal penicillopepsin, we have analyzed the crystal structures of penicillopepsin complexed with these three inhibitors. On the basis of the high-resolution structures, this study explains the differences in their binding ability to the fungal aspartyl proteinase and the conformational changes upon binding of these inhibitors.

Methods

Design, Synthesis, and Analysis of Inhibitors. The macrocyclic peptidyl phosphonate **1** {methyl[cyclo-7[(2*R*)-((*N*-valyl)amino)-2-(hydroxyl-(1*S*)-1-methyoxycarbonyl-2-phenylethoxy)phosphinyloxyeth-

(10) Fraser, M. E.; Strynadka, N. C. J.; Bartlett, P. A.; Hanson, J. E.; James, M. N. G. *Biochemistry* **1992**, *31*, 5201−5214.
(11) Fujinaga, M.; Chernaia, M. M.; Tarasova, N. I.; Mosimann, S. C.; James, M. N. G. *Protein Sci.* **1995**, *40*, 960−972.
(12) Suguna, K.; Padlan, E. A.; Bott, R.; Boger, J.; Parris, K. D.; Davies, D. R. *Proteins* **1992**, *13*, 195−205.
(13) Bailey, D.; Cooper, J. B.; Veerapandian, B.; Blundell, T. L.; Atrash, B.; Jones, D. M.; Szelke, M. *Biochem. J.* **1993**, *289*, 363−371.
(14) Iliadis, G.; Zundel, G.; Brzezinski, B. *FEBS Lett.* **1994**, *352*, 315−317.
(15) Iliadis, G.; Brzezinski, B.; Zundel, G. *Biophys. J.* **1996**, *71*, 2840−2847.
(16) Oldziej, S.; Ciarkowski, J. *J. Comput.-Aided Mol. Des.* **1996**, *10*, 583−588.

Table 1. Crystal Data for Phosphonate Inhibitor Complexes with Penicillopepsin

	penicillopepsin complexed to			
	1	Cryo_**1**[a]	**2**	**3**
space group	*C*2	*C*2	*C*2	*C*2
cell dimensions				
a (Å)	97.88	96.33	97.38	97.24
b (Å)	46.64	46.27	46.55	46.63
c (Å)	66.59	64.59	66.19	65.87
β (deg)	116.14	115.10	115.78	115.95
detector	DIP image plate detector	SIEMENS multiwire detector	SIEMENS multiwire detector	SIEMENS multiwire detector
X-rays Cu Kα (λ)	1.5418 Å	1.5418 Å	1.5418 Å	1.5418 Å
temp	room	110 K	room	room
resolution (Å)	20.0−1.5	40.0−1.25	40.0−1.5	37.0−1.5
total meas.	162 263	203 415	213 907	205 980
unique reflns	38 650	58 629	40 665	39 118
reflns (>2σ)	36 649	55 829	37 137	35 565
R_{merge}[b] (%)	7.9	6.0	8.4	8.9
completeness	1.55−1.50 (Å) 77.55%	1.29−1.25 (Å) 40.47%	1.55−1.50 (Å) 78.94%	1.55−1.50 (Å) 69.82%
	20.0−1.50 (Å) 89.18%	40.0−1.25 (Å) 82.22%	40.0−1.50 (Å) 94.74%	37.0−1.50 (Å) 91.72%

[a] Cryo_**1** = **1** at 110 K. [b] $R_{merge} = \Sigma(I_i - \bar{I})/\Sigma I_i$, where I_i represents the intensities of the multiply measured reflections and $\bar{I}$ is their average value.

yl]-1-naphthaleneacetamide] sodium salt} along with two acyclic comparison compounds **2** and **3** (Figure 1) were synthesized and have been evaluated as inhibitors of penicillopepsin. The exact details of the design, synthesis, evaluation of inhibitor constants and the NMR analysis have been described previously.[9]

Crystallization and Data Collection. Samples of penicillopepsin were kindly provided by Professor T. Hofmann, University of Toronto. The solutions of the complexes were prepared by mixing the enzyme with each inhibitor in water. The molar ratio of penicillopepsin to inhibitor was 1:6. Crystals were obtained according to crystallization conditions similar to those described previously.[10] A macro-seeding method was used to optimize the quality of crystals. Normally, the crystals will reach an adequate size (0.51 × 0.45 × 0.48) mm^3 after two or three rounds of macro-seeding procedures within 1 month. All new seeds with the typical morphology of the crystals of penicillopepsin complexed with inhibitor molecules[17] were chosen for the next cycle of macro-seeding.

The first data set of penicillopepsin complexed with **1** was collected from one crystal at room temperature on a DIP 2030H image plate detector (Mac Science Co., Ltd.), using double-mirror focusing optics and Cu Kα radiation generated with a Rigaku rotating anode generator RU-200BH operating at 45 kV and 75 mA. The distance from the crystal to the detector was set to 70 mm. Only 140 images at 1.0 degree intervals were collected because the crystal decayed after 2 days of exposure. The data were processed and reduced with the programs Denzo and Scalepack.[18] The resolution of this data set was 1.5 Å with completeness of 89.18% (Table 1).

The intensity data for each of the acyclic inhibitors **2** and **3** bound to penicillopepsin were collected on a Siemens X1000 area detector mounted on a Siemens rotating anode system operating at 45 kV and 85 mA. The detector was positioned 10 cm away from the crystal and was swung to a 2θ angle of 38°, giving a maximum resolution of 1.45 Å at the edge of the detector. In both cases, the 2θ angle needed also to be set to 20° to collect the data at low resolution. The data collection strategy was based upon protocols already reported.[19] All data collected on the Siemens X1000 area detector were processed with the program Xengen.[20] The crystals of each complex could last through 2 weeks of exposure to the graphite-monochromated Cu Kα radiation without significant decay. The entire data set was achieved from one crystal for each complex. The data sets of the three complexes collected at room temperature are of similar quality and all have the same resolution of 1.5 Å (Table 1).

The low-temperature data for penicillopepsin complexed with **1** were obtained on the Siemens X1000 area detector from one crystal flash frozen in the nitrogen stream of an Oxford Cryostream cooler at 110 K.[21] The cryoprotection solution through which the crystal was quickly transferred contained 25% glycerol, 65% saturated $(NH_4)_2SO_4$ buffered by 0.1 M $NaC_2H_3O_2$ at pH = 4.4. The frozen crystal gave very strong diffraction spots at the edge of the chamber when the detector was swung to a 2θ angle of 55°, namely, the resolution reaches 1.15 Å with Cu Kα radiation. These are crystals of one of the largest proteins currently known to diffract to such high resolution with a rotating anode generator. However, the spacial constraints of the Siemens X1000 system and the design of the goniometer hindered us from collecting a complete data set to 1.15 Å resolution. The final data were 82.22% complete at 1.25 Å and scaled with an overall R_{merge} on intensity of 6.0% (Table 1). The cell dimensions of the frozen crystals shrink by 1.5 Å along the *a*-axis, 2.0 Å along the *c*-axis, and about 1.0° in the β angle.

Structural Refinements. Difference electron density maps for complexes **1**−**3** were computed with coefficients $|F_o| - |F_c|$ and calculated phases, α_c, from the refined complexes of penicillopepsin with other phosphonate-containing inhibitors[10] using programs from the CCP4 package.[22] Only the atoms of penicillopepsin were used in the initial phase calculation. The initial coordinates of the three inhibitors were derived from the clear electron density contours of these difference maps in the active site of the enzyme using the modeling program Turbo-Frodo 5.5.[23] The initial refinement stages for the three inhibitors included positional refinements and *B*-factor refinements with the program X-PLOR.[24] Solvent molecules were built into the difference density maps and then inspected during the subsequent refinement cycles. There was one SO_4^{2-} ion identified in each complex. The occupancies of atoms in residues having alternate conformations were refined in the last stages of refinement during several cycles of coordinate refinement using the program TNT.[25]

(17) James, M. N. G.; Sielecki, A.; Salituro, F.; Rich, D. H.; Hofmann, T. *Proc. Natl. Acad. Sci. U.S.A.* **1982**, *79*, 6137−6141.

(18) Otwinowski, Z.; Minor, W. *Methods Enzymol.* **1996**, *276*. Carter, C. W., Jr., Sweet, R. M., Eds.; Academic Press: New York, London; pp 307−326.

(19) Derewenda, Z.; Helliwell, J. R. *J. Appl. Crystallogr.* **1989**, *22*, 123−137.

(20) Howard, A. J.; Gilliland, G. L.; Finzel, B. C.; Poulos, T. L.; Ohlendorf, D. H.; Salemme, F. R. *J. Appl. Crystallogr.* **1987**, *20*, 383−387.

(21) Cosier, J.; Glazer, A. M. *J. Appl. Crystallogr.* **1986**, *19*, 105−107.

(22) Collaborative Computational Project, Number 4. *Acta Crystallogr.* **1994**, *D50*, 760−763.

(23) Roussel, A.; Cambillau, C. In *Silicon Graphics geometry partners directory;* Silicon Graphics: Mountain View, CA, 1991.

(24) Brünger, A. T. *X-PLOR υ3.1 A System for X-ray Crystallography and NMR*; Yale University Press: New Haven, CT, and London, 1992.

Table 2. Refinement Statistics for the Penicillopepsin−Phosphonate Inhibitor Complex Structures

parameters	**1**	Cryo_**1**[a]	**2**	**3**
resolution range (Å)	20.0−1.5	40.0−1.25	40.0−1.5	37.0−1.5
reflns ($>2\sigma$)	36 649	55 829	37 137	35 565
R_{cryst} (all data)[b] (%)	15.9	15.0	16.0	15.2
R_{free}[b] (%)	19.8	19.7	20.3	21.4
R_{cryst} ($F > 2\sigma$)[b] (%)	15.4	14.5	15.1	14.1
R_{free}[b] (%)	19.3	19.2	19.5	20.4
no. of protein atoms (+sugar)	2397	2398	2400	2396
no. of inhibitor atoms	45	39	38	38
no. of water molecules	281	512	323	338
no. of SO_4^{2-} ions	1	1	1	1
rms deviations from ideal bond lengths (Å)	0.010	0.014	0.007	0.010
bond angles (deg)	1.305	1.454	1.287	1.345
rms coordinate error (Å)	0.15	0.14	0.19	0.19
uncertainty in rms error	0.0020	0.0015	0.0053	0.0051
average *B*-factor for				
enzyme	15.6	8.5	14.0	13.9
inhibitor	17.1	8.0	16.8	27.9
H_2O	36.3	25.6	36.1	39.0
SO_4^{2-}	58.7	34.7	51.2	50.3
residues with two alternate conformations	9Thr, 60Ser, 67Ser, 145Lys, 147Ser, 174Lys, 202Ser, 222Asp, 297Ile, phenyl ring of inhibitor	9Thr, 74Ser, 79Ser, 89Ser, 147Ser, 174Lys, 197Ser, 202Ser, 257Ser	9Thr, 74Ser, 79Ser, 155Val, 202Ser, 250Ser, 257Ser, 297Ile	9Thr, 72Ser, 74Ser, 176Thr, 202Ser, 297Ile

[a] Cryo_**1** = **1** at 110 K. [b] $R = \Sigma||F_o| - |F_c||/\Sigma|F_o|$, where R_{free} is calculated for a randomly chosen 10% of reflections, and R_{cryst} is calculated for the remaining 90% of reflections used for structure refinement.

The frozen crystals of **1** bound to penicillopepsin have relatively large unit cell dimension changes and are not isomorphous with the crystals of the three complexes at room temperature. Initially, rigid-body refinement, energy minimization, and simulated annealing refinement with X-PLOR[24] were used exclusively for the low-temperature model of the complex with **1** to improve the *R*-factor and the appearance of the electron density map. Later refinement strategies were similar to those for complexes at room temperature.

Ideal geometries for the groups that were not included in X-PLOR or TNT libraries were chosen from the Cambridge Structural Database.[26] Statistics of the structural refinements are listed in Table 2. The data and the refined atomic coordinates have been submitted to the Brookhaven Protein Data Bank.[27,28] The codes are 2WEA (**1** bound to penicillopepsin at 110 K), 2WEB (**2** bound to penicillopepsin), 2WEC (**3** bound to penicillopepsin), and 2WED (**1** bound to penicillopepsin at room temperature).

Results

The present models of phosphonate-containing macrocyclic and acyclic inhibitors bound to penicillopepsin were obtained from the high-resolution structural refinements, three at 1.5 Å and one at 1.25 Å. The reasonable crystallographic residuals (*R*-factor and R_{free}) show the close agreement between the calculated and observed structure factor amplitudes. The stereochemical parameters are in excellent agreement with the parameter set derived by Engh and Huber.[29] In addition to the tetrahedral character of each phosphonate-containing inhibitor, the macrocyclic character of **1**, the acyclic branched shape of **2**, and the acyclic linear shape of **3** were all unambiguously revealed in the initial difference maps and the subsequent electron-density maps (Figure 2).

The average values of the *B*-factors of each inhibitor at room temperature are 17.1 Å^2 (**1**), 16.8 Å^2 (**2**), and 27.9 Å^2 (**3**), showing that all inhibitors are tightly bound in the vicinity of the active site of enzyme. The model of **1** at 110 K has lower average *B*-factors, probably due to the reduced thermal motion of the atoms at low temperature. Thus, there is a high degree of confidence in the models of inhibitors in the vicinity of the active site.

Discussion

Binding Interactions between Penicillopepsin and Inhibitor 1. Contact distances for possible hydrogen bonds are listed in Table 3. The carbonyl oxygen of P3, OI (atom labeling is given in Figure 1), receives a hydrogen bond from the main chain NH of Thr217 in penicillopepsin (Figure 3). This kind of main chain hydrogen bond involving the P3 residues is frequently seen in many other complexes of aspartic proteinases with inhibitors.[5,10,17,33−38] The ordered solvent molecule W16 serves as a hydrogen-bonded bridge between OI and the main chain nitrogen atom of Leu218, thereby helping to fix the N-terminal part of the inhibitor.

(25) Tronrud, D. E. *Acta Crystallogr.* **1992**, *A48*, 912−916.
(26) Allen, F. H.; Kennard, O. *Chem. Des. Automat. News* **1993**, *8*, 1, 31−37.
(27) Abola, E. E.; Bernstein, F. C.; Bryant, S. H.; Koetzle, T. F.; Weng, J. In *Crystallographic Databases−Information Content, Software Systems, Scientific Applications*; Allen, F. H., Bergerhoff, G., Sievers, R., Eds.; Data Commission of the International Union of Crystallography: Bonn/Cambridge/Chester, 1987; pp 107−132.
(28) Bernstein, F. C.; Koetzle, T. F.; Williams, G. J. B.; Meyer, E. F., Jr.; Brice, M. D.; Rodgers, J. R.; Kennard, O.; Shimanouchi, T.; Tasumi, M. *J. Mol. Biol.* **1977**, *112*, 535−542.
(29) Engh, R. A.; Huber, R. *Acta Crystallogr.* **1991,** *A47*, 392−400.
(30) Kraulis, P. J. *J. Appl. Crystallogr.* **1991**, *24*, 946−950.
(31) Esnouf, R. *J. Mol. Graphics* **1997**, *15*, 133−138.
(32) Schechter, I.; Berger, A. *Biochem. Biophys. Res. Commun.* **1967**, *27*, 157−162.
(33) Davies, D. R. *Annu. Rev. Biophys. Biophys. Chem.* **1990**, *19*, 189−215.
(34) Suguna, K.; Padlan, E. A.; Smith, C. W.; Carlson, W. D.; Davies, D. R. *Proc. Natl. Acad. Sci. U.S.A.* **1987**, *84*, 7009−7013.
(35) Cooper, J.; Foundling, S.; Hemmimgs, A.; Blundell, T.; Jones, D. M.; Hallett, A.; Szelke, M. *Eur. J. Biochem.* **1987**, *169*, 215−221.
(36) Cooper, J. B.; Foundling, S. I.; Blundell, T. L.; Boger, J.; Jupp, R. A.; Kay, J. *Biochemistry* **1989**, *28*, 8596−8603.
(37) Foundling, S. I.; Cooper, J.; Waston, F. E.; Cleasby, A.; Pearl, L. H.; Sibanda, B. L.; Hemmings, A.; Wood, S. P.; Blundell, T. L.; Valler, M. J.; Norey, C. G.; Kay, J.; Boger, J.; Dunn, B. M.; Leckie, B. J.; Jones, D. M.; Atrash, B.; Hallett, A.; Szelke, M. *Nature* **1987**, *327*, 349−352.
(38) Sali, A.; Veerapandian, B.; Cooper, J. B.; Foundling, S. I.; Hoover, D. J.; Blundell, T. L. *EMBO J.* **1989**, *8*, 2179−2188.

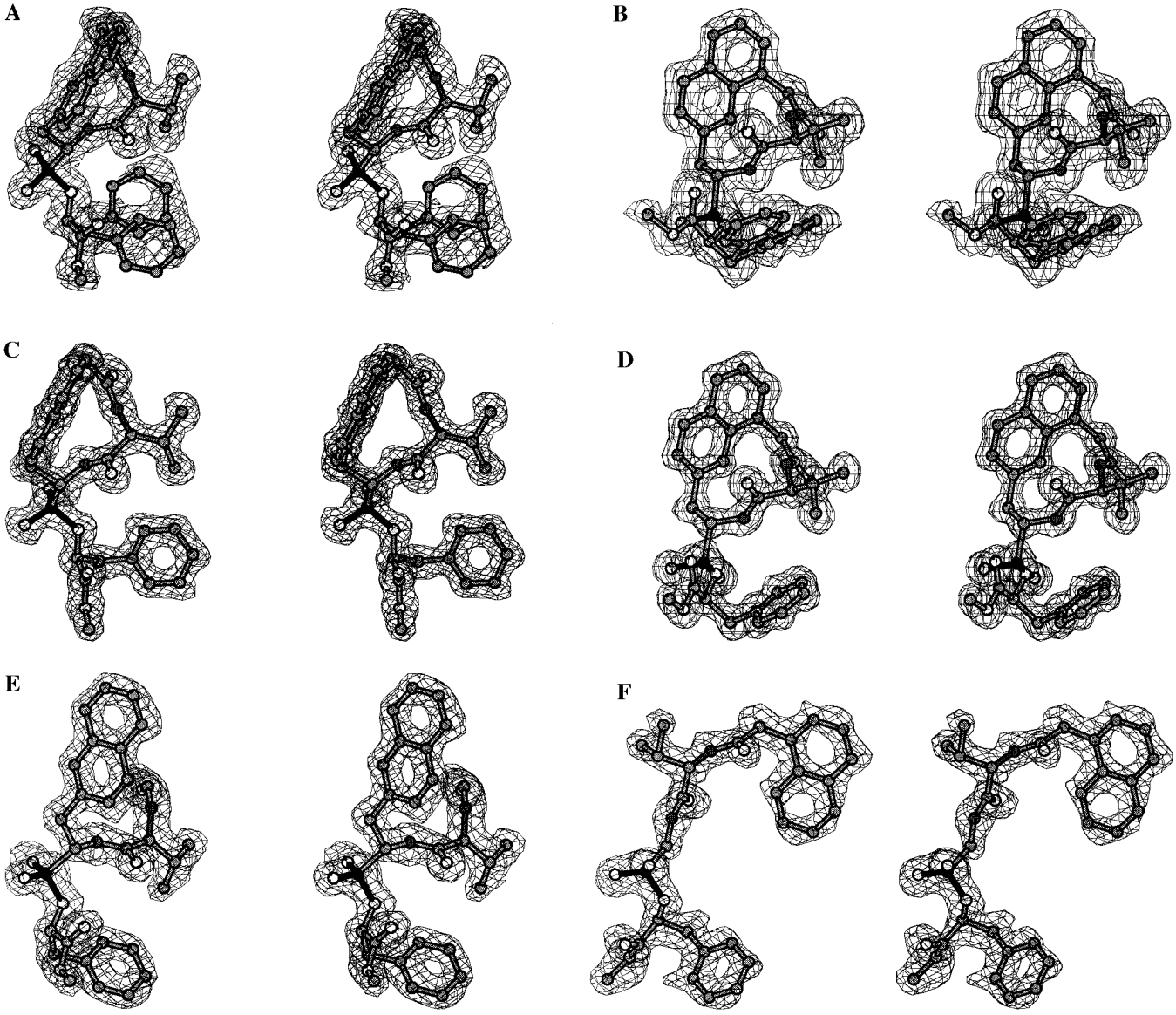

Figure 2. The final $2|F_o| - |F_c|$ electron density map of each inhibitor in stereo. The maps were contoured at 1σ. (A, B) Two views of **1**. (C, D) Two views of Cryo_**1**. (E) View of **2**. (F) View of **3**. This figure and Figures 3−11 were produced using the program Molscript[30] with Bobscript[31] extensions.

The P2 Val CO receives one hydrogen bond from the main-chain NH of Asp77 and another one from Gly76NH. Both of these two hydrogen bonds are provided by the flap in the closed conformation of the inhibited form of penicillopepsin.[17]

The interactions between the oxygen atoms of the carboxyl groups of Asp33, Asp213, and the phosphonyl oxygen atoms of the macrocyclic inhibitor **1** are very similar to those in other phosphorus-containing peptide inhibitors that have been described in detail previously.[10] Besides those interactions with the active site residues Asp33 and Asp213, the P1 residue has an additional contact with Thr216 Oγ1, forming a hydrogen bond with its NH. The naphthalene group that is the linker between P1 and P3 is located in a rather hydrophilic region containing Tyr75, Ser79, Asp77, Gly215, and water W135. The atoms of the naphthalene make contacts of less than 3.6 Å with atoms of these residues, most of which are on the flap, and with the solvent molecule.

The carbonyl oxygen atom of P1′ forms a hydrogen bond to the NH of Gly76 on the flap of penicillopepsin; this is a common interaction among the several aspartic proteinases complexed with inhibitors.[5,10,33−38] The P1′ Phe has two alternate conformations of the phenyl ring. In one conformation, the phenyl ring points to the predominantly hydrophobic S1′ pocket similar to the P1′−S1′ interaction in the phosphorus-containing peptide inhibitor.[10] In the other conformation, the phenyl ring is within 3.6 Å of solvent molecules W30 and W206.

The ester oxygen of the methyl ester, structurally equivalent to the P2′ NH, forms a strong hydrogen bond with water molecule W30. W30 serves as the second hydrogen-bond bridge, linking the ester oxygen to the carbonyl oxygen of Gly35, thereby stabilizing the C-terminal part of **1**.

Comparison of the Complex of Penicillopepsin with Inhibitor 1 and the Complex with the Phosphonate Pentapeptide Inhibitor 4. The macrocyclic inhibitor of penicillopepsin, **1**, is a "second-generation" product of molecular modeling, designed to reduce the conformational flexibility of the ligand. The design was based upon the X-ray structure of **4** bound to penicillopepsin.[10] One conformational feature of **4** bound to penicillopepsin is the proximity of the side chains on alternate residues (P3 and P1, P2 and P1′). The naphthalene

Table 3. Contact Distances (Å) for Possible Hydrogen Bonding in Active Sites of Complexes

	atoms involved		distance (Å)			
site	inhibitor[a]	penicillopepsin	**1**	Cryo_**1**[b]	**2**	**3**
P3	CO	Thr217 NH	3.07	2.95	3.33	
		H_2O16 O	2.93	2.85	2.61(H_2O49)[c]	
		H_2O312 O				3.08
		H_2O294 O				3.38
P2	NH	H_2O389 O		3.12		
		Thr217 Oγ1				3.06
	CO	Asp77 NH	3.15		3.21	
		Gly76 NH	3.26		3.20	
		H_2O388 O		2.87		
		H_2O389 O		2.95		
		Thr217 NH				3.05
		H_2O50 O				2.51
P1	NH	Thr216 Oγ1	3.19	3.06	3.37	
		Asp77 Oδ2				2.91
	PO	Asp33 Oδ1	(3.78	3.59	3.71)[d]	
		Asp33 Oδ2	3.18	3.16	3.07	
		Asp213 Oδ1	2.70	2.62	2.59	
		Asp213 Oδ2	2.81	2.92	2.88	
		H_2O103 O				2.77
		H_2O25 O				2.67
	POH	Asp33 Oδ1	2.55	2.49	2.51	
		Asp33 Oδ2	(3.36	3.33	3.30)[d]	
		Asp77 Oδ1				3.17
		Asp77 Oδ2				3.25
		Asp77 NH				2.88
		H_2O263 O		2.86		
P1′	CO	Gly76 NH	2.92		2.99	3.05
	OP	H_2O324 O				3.10
P2′	OMe[e]	H_2O30 O	2.33	3.24	3.17(H_2O227)[c]	

[a] The nomenclature of Schechter and Berger[32] is used to describe the interactions of enzyme and inhibitors. P*n* and P*n*′ denote residues on either side of the scissile bond, by definition between P1 and P1′. S*n* and S*n*′ denote the corresponding binding pockets in the enzyme. [b] Cryo_**1** = **1** at 110 K. [c] The number for the corresponding solvent molecule. [d] The stereochemistry of these interactions is inconsistent with hydrogen bonding, but the distances are included here for completeness. [e] OMe = methyl ester.

group serves as a linker between P1 and P3 residues in the macrocyclic inhibitor **1**.[9] It is important to compare the bound conformation of **1** with its "parent model", **4**.

The macrocylic inhibitor **1** basically adopts a similar conformation to that of the linear inhibitor **4**, with a rms displacement of 0.458 Å for the common atoms (Figure 4 and Table 4). The largest differences are found in the following regions: the methyl ester carbon atoms at the C-terminus, where the ϕ angles of the P1′ residues have a difference of 21° (Table 5), and the two methylene units, C11 and C13, where the ω angle of P1 is 127° in **1** compared with 147° in **4**. The methylene units can be thought of as a pair of hinges, allowing movement of the naphthalene ring. The change of angle χ_2 of P1 only reflects the different side chains in the two inhibitors. The phosphonyl group is shifted by ~0.2Å toward the C-terminus of the inhibitor binding site of penicillopepsin. The very short hydrogen bond (2.4Å) from the *pro-S* phosphonate oxygen to Asp33 Oδ1 in the **4** complex is a little longer, 2.55 Å, in the **1** complex. In addition to that, the hydrogen-bonding interactions involving main chain atoms of the inhibitors exhibit some differences. The hydrogen bond from P3 (Val in **4**) NH to Thr217 Oγ1 is lost in the **1** complex, for there is no main chain nitrogen at P3. As well as the two hydrogen bonds to the P2 carbonyl oxygen from Gly76 NH and Asp77 NH on the flap, **4** has a third hydrogen bond connecting **4** (Val in P2) NH and Asp77 Oδ1. The **1** complex does not have this one. The interactions of P1 are mostly consistent between **4** and **1**, with the exception that P1 NH donates the proton to a different acceptor, to Thr216 Oγ1 in the **1** complex and to Gly215 carbonyl oxygen in the **4** complex.

Looking at the penicillopepsin molecule in the **4** and **1** complexes, the regions that constitute the S3 binding pocket undergo minor conformational changes. The side chains of Gln111, Glu15, and Glu16 adopt different conformations to avoid too close contact with the naphthalene ring. The overall rms difference, based upon 1292 main chain atoms, is 0.273 Å.

A number of reasons can be invoked to explain the 3.4 kcal/mol difference in binding affinity between **4** (K_i = 2.8 nM) and **1** (K_i = 800 nM). More hydrophobic surface is buried on binding the pentapeptide (716 Å^2) than the macrocycle (554 Å^2) (Table 6), and there are more hydrogen-bonding interactions between the enzyme and the former inhibitor (11) than the latter (9). The flap over the enzyme active site adopts a more open, and presumably higher energy, conformation in the complex with **1** in order to accommodate the puckered conformation of the naphthalene-bridged macrocycle.

Binding Interactions between Penicillopepsin and 1 at 110 K. A comparison of the coordinates of the two penicillopepsin structures complexed with the macrocyclic inhibitor **1**, one at room temperature and one at 110 K, gives a rms displacement of 0.399 Å for 1248 main chain atoms, omitting the flap, Ser72−Ser82 (Figure 5A, Table 4). The flap has moved away from the inhibitor to a more open conformation which is very unusual for complexes of penicillopepsin with inhibitors.[5,10,17] Gly76 Cα has the largest displacement: 3.73 Å. The conformation of the flap at 110 K is similar to that of native penicillopepsin (Figure 5B). Packing of one molecule with a second molecule related by the crystallographic 2-fold symmetry operation, $1-x$, y, $1-z$, involves contacts in the region of the flap.[42] The movement of the flap away from the inhibitor at 110 K allows for more intermolecular contacts along the flap than are present in the structures with the closed conformation at room temperature (Table 7). Before flash freezing, the crystals were transferred to cryoprotectant containing 65% $(NH_4)_2SO_4$ and 25% glycerol, but since the transfer was very fast, it is unlikely that the cryoprotectant diffused into the crystals. We believe that the changes in the structure between room temperature and the cryotemperature are due to the temperature change. The frozen crystals of penicillopepsin complexed with **1** have a much smaller cell volume of 260 726 Å^3, compared to the volume of the room-temperature crystals 271 737 Å^3. The region of Gly235−Gly244, which packs against the disordered segment of Pro276−Thr282, also exhibits obvious conformational change. The Cα of Asn241 has shifted 1.926 Å from the room-temperature position. Other regions, such as Ser109−Glu114, Pro276−Thr282, and Ser291−Phe295, show smaller but significant conformational differences. These regions all border the entrance to the substrate binding cleft.[42]

The conformation of the macrocyclic inhibitor **1** and the binding interactions also exhibit obvious differences between the room temperature and the 110 K structures. Applying the orientation matrix resulting from the superposition of the penicillopepsin structures complexed with **1** at the different temperatures, the comparison of the transformed inhibitor coordinates yielded a rms difference of 0.370 Å (not including the phenyl ring) (Table 4). The maximum displacement is 1.276

(39) Richards, F. M. *Ann. Rev. Biophys. Bioeng.* **1977**, *6*, 151−176.
(40) Connolly, M. L. *Science* **1983**, *221*, 709−713.
(41) Connolly, M. L. *J. Appl. Crystallogr.* **1983**, *16*, 548−558.
(42) James, M. N. G.; Sielecki, A. R. *J. Mol. Biol.* **1983**, *163*, 299−361.

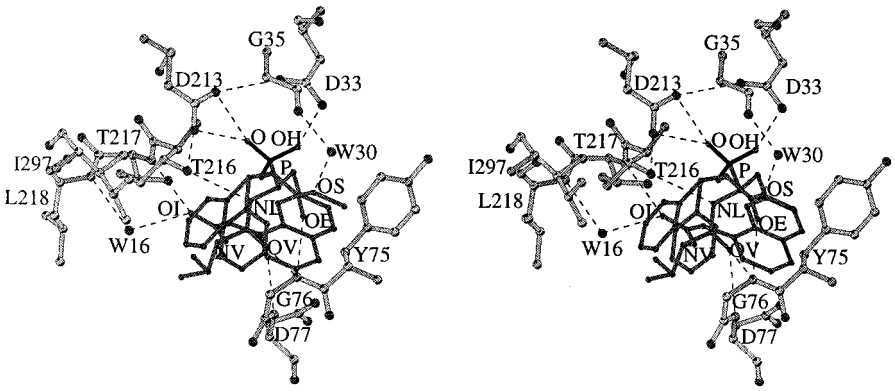

Figure 3. Stereoview of the hydrogen bonding with **1** in the active site. The inhibitor is presented in black sticks; the enzyme is in gray sticks; hydrogen bonds are shown by dashed lines.

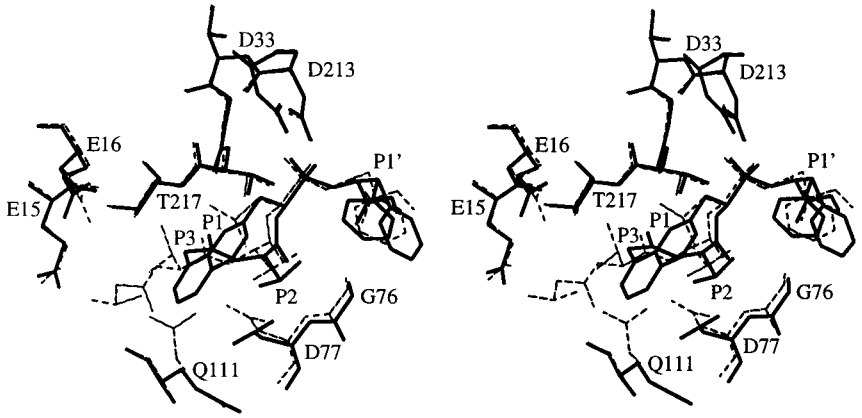

Figure 4. Superposition of penicillopepsin complexed with **1** and penicillopepsin complexed with **4**; **1** and residues in the active site are represented by solid lines. The equivalent penicillopepsin residues and **4** are represented by dashed lines.

Table 4. Comparison of the Various Molecular Complexes of Inhibitors with Penicillopepsin, Main-Chain[a] Atoms rms (Å)

	1	Cryo_**1**[b]	**2**	**3**	**4**[c]
native	0.295	0.306	0.222	0.204	0.198
1		0.399	0.205	0.231	0.273
Cryo_**1**	0.370(33)		0.305	0.296	0.304
2	0.309(22)	0.303(28)		0.159	0.172
3	2.088(32)	2.030(32)	2.135(21)		0.185
4	0.458(25)	0.353(31)	0.232(29)	0.205(12)	

[a] The upper right triangular portion of this matrix has the rms values that result from least-squares fitting of the 1292 main-chain atoms of penicillopepsin from each complex in a pairwise fashion. For those comparisons that involve the native structure or the Cryo_**1** complex, the nine residues (36 atoms) that comprise the flap (Ile73−Ala81) have been omitted from the calculation. The lower triangular portion of the matrix gives the rms differences that result from the best fit of the common atoms of the inhibitors when compared in a pairwise fashion. The numbers in parentheses are the number of atoms in the least-squares fitting. [b] Cryo_**1** = **1** at 110 K. [c] **4** = IvaVVL^{P}(O)FOMe.

Å at the ester carbon of the methyl ester at the C-terminus of **1** (Figure 5A). The naphthalene ring, the P1 to P3 linker, is rotated toward the flap, accompanying the movement of the flap. The ω angle of the P1 residue has changed by 23° from 127° at room temperature to 150° at 110 K (Table 5). The P1′ residue undergoes a much larger change. The ϕ angle of P1′ is −120° at 110 K but −92° at room temperature. The phenyl side chain of P1′ is very flexible at room temperature. The solution conformation studies on the macrocyclic ring system by NMR also show multiple conformations of the P1′ residue at room temperature.[9] However, the phenyl ring has only one conformation in the electron density map (Figure 2C,D) calculated from the data at 110 K. That conformation lies close to one of the two alternate ones at room temperature (Table 5, Figure 5A). The average *B*-factor of the phenyl side chain of P1′ is 8.64 Å^2 at 110 K and 20.30 Å^2 and 18.66 Å^2 for the two alternate conformations at room temperature. It is very possible that the side chain of P1′ is dynamically disordered at room temperature. The conformation frozen at 110 K is presumably the conformation with the lowest energy.

The movement of the flap affects the binding interactions between penicillopepsin and the macrocyclic inhibitor **1**. Since the flap moves away from the inhibitor, Asp77 NH and Gly76 NH are located too far away to form the normal hydrogen bonds with the carbonyl oxygen atom O of P2. Two ordered solvent molecules W388 and W389 (Figure 6, Table 3) take the place of the NH of Asp77 and the NH of Gly76 in forming hydrogen bonds with the carbonyl oxygen of P2. W389 forms another hydrogen bond with the amide NH of P2. The hydrogen bond between solvent molecule W389 and the main chain nitrogen of P2 is exclusive to the structure at 110 K; no similar hydrogen bonds are found in the complexes of **1**−**3** at room temperature. Asp77 Oδ2 helps to stabilize the water W389 by accepting a hydrogen bond from it. Ordered solvent molecules W389, W267, W190, and W407 lie within hydrogen bonding distance from one and other and form a solvent channel along the entrance to the binding cleft. Water W407 is fixed by a hydrogen bond with Gln111 Nγ2. With the shift of Tyr75 of the flap, a third hydrogen-bonded water bridge is formed by W263 between the *pro-R* oxygen atoms of the phosphonyl group and the OH of Tyr75. Two other hydrogen-bonding bridges connected by waters W16 and W30 are the same as those at room temperature.

Table 5. Conformational Angles (deg) of Inhibitors Bound to Penicillopepsin

conformational angles[a]		**1**A[b]	**1**B[b]	Cryo_**1**[c]	**2**	**3**	**4**[d]
P3							
ω	C11−C12−NV−CAV	168		165		176	179
χ_2	C11−C1−C2−C3	−177		−178		−180	
P2							
ϕ	C12−NV−CAV−CV	−116		−118	−128	−115	−132
ψ	NV−CAV−CV−NL	91		94	73	159	99
ω	CAV−CV−NL-C14	−174		−172	−176	−180	−180
χ_1	NV−CAV−CBV−CV1	−162		−178	−152	46	−176
P1							
ϕ	CV−NL-C14−P	−136		−139	−118	−170	−123
ψ	NL-C14−P−OP	69		73	71	−132	73
ω	C14−P−OP−CA	127		150	141	−89	147
χ_1	NL-C14−C13−C8	−62		−61	−53		−48
χ_2	C14−C13−C8−C9	−97		−93	−36		159
P1′							
ϕ	P−OP−CA-C	−92		−120	−110	−96	−113
ψ	OP−CA-C−OS	175		−179	−171	167	174
ω	CA-C−OS−CS	−160		−172	−168	−173	−178
χ_1	OP−CA-CB−CG	36	86	66	63	67	63
χ_2	CA-CB−CG-CD1	120	77	103	101	66	96

[a] The atom numbering is shown in Figure 1. [b] Two alternative conformations of **1**. [c] Cryo_**1** = **1** at 110 K. [d] **4** = IvaVVL^{P}(O)-FOME.

Table 6. Solvent-Accessible Surface Area (Å^2)[a]

	uncomplexed			complexed				
inhibitor	hydrophilic surface area	hydrophobic surface area	total	hydrophilic surface area	hydrophobic surface area	total	Δ[b]	(%)
1	159	564	724	4	164	170	554	76
Cryo_**1**[c]	169	564	732	11	186	197	535	73
2	172	585	757	4	133	137	620	82
3	184	651	834	33	139	172	662	79
4	192	673	866	26	124	150	716	83

[a] Calculated according to the algorithm of Richards[39] using a program developed by Connolly.[40,41] [b] Δ is the difference in the total solvent-accessible surface areas calculated for the uncomplexed and complexed forms of the inhibitors. [c] Cryo_**1** = **1** at 110 K.

Due to the movement of the flap and the redistribution of ordered solvent molecules, there are two more hydrogen-bonding interactions between solvent molecules in the active site and macrocyclic inhibitor **1** (Table 3).

Complex of the Acyclic Branched Inhibitor 2 Bound to Penicillopepsin. Inhibitor **2** differs from macrocycle **1** by substitution of two hydrogen atoms for the methylene group, C11, which connects the naphthalene ring with the carbonyl carbon at P3. The naphthalene unit remains part of the structure as the P1 side chain. The acyclic comparison compound **2** and its companion **3** were intended to bind to penicillopepsin in the same way as the macrocycle **1** and thus enable the effect of the bridging unit in limiting conformational flexibility to be distinguished from its contribution to binding as a hydrophobic moiety.[9]

The electron-density map for **2** revealed a large difference in the position of the naphthalene ring (Figure 2E). The bound acyclic **2** adopts a more open conformation by rotating the χ_2 angle of P1 about 60° (Table 5). The χ_2 angle in **2** is close to −30°, an unfavorable angle for an aromatic ring, as known from the database of Phe, Tyr, and Trp residues. For **1**, this angle is about −90°, the most favorable angle in Phe, Tyr, and Trp residues. A comparison of the 22 atoms in common between **2** and **1** (omitting the naphthyl and phenyl rings), when their positions are overlapped as in Cryo_**1** (**1** at 110 K) to **1**, yields a rms displacement of 0.309 Å (Table 4). The largest differences can be found at the C-terminal atom OI with a 0.572 Å shift and at the N-terminus (Figure 7). The large rotation of the torsion angle χ_2 brings the P1 residue pointing to the S1 pocket and allows a hydrophobic interaction between the naphthyl ring and the phenyl ring of Phe112, as well as displacing the ordered solvent molecule W135 from the S1 pocket.

However, a comparison of the penicillopepsin molecule in the **2** complex with that in the **1** complex shows only minor differences with a rms displacement of 0.205 Å (with all main chain atoms) (Table 4). The binding interactions between penicillopepsin and the acyclic branched inhibitor **2** are very similar to those in the **1** complex. Solvent molecules W49 and W227 (Figure 8) are the water molecules corresponding to W16 and W30, respectively, in the structure of the **1** complex, but the distance between water W49 and Leu218 NH is 3.34 Å, longer than that for W16. The openness of the macrocycle lowers the inhibition ability of **2**, whose inhibition constant K_i is 7.6 μM.

Complex of the Acyclic Linear Inhibitor 3 Bound to Penicillopepsin. By analogy to the other acyclic inhibitor, the linear analogue **3** differs from the macrocycle by removal of the methylene group, C13, on the other side of the naphthalene ring.[9] Since the aromatic group is part of the P3 residue instead of P1, the molecule is less highly branched and therefore subject to less conformational constraint.

Comparison of the Complex with 3 and the Complex with 1. A comparison of the structure of penicillopepsin in the **3** complex with that in the **1** complex shows that the two differ only in minor respects, with a rms difference of 0.231 Å for all the main chain atoms (Table 4). However, the superposition of the bound conformations of **3** and **1**, based upon the superposition of the two penicillopepsin structures, yields a very large rms displacement of 2.08 Å for the 32 atoms common to the two inhibitors, not including the phenyl ring (Table 4). Indeed, the conformation that **3** adopts when it is bound to

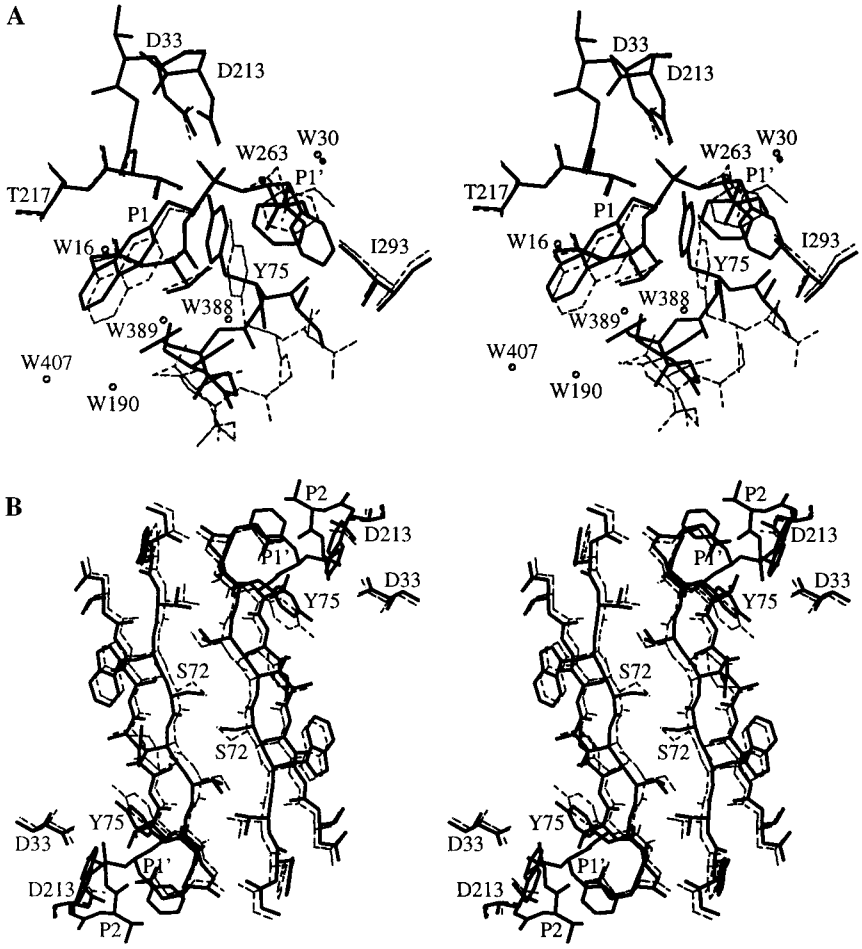

Figure 5. (A) Superposition of penicillopepsin complexed with **1** and penicillopepsin complexed with Cryo_**1**. **1** and residues in the active site are represented by solid lines; the solvent molecules of this complex are represented by filled circles. The equivalent penicillopepsin residues and Cryo_**1** are represented by dashed lines; the solvent molecules, by open circles. (B) Superposition of native penicillopepsin and the complex with Cryo_**1**. **1**, residues 68 to 84 of penicillopepsin in the complex, and the active site aspartyl residues are represented by solid lines. The equivalent residues of uncomplexed penicillopepsin are represented by dashed lines. The view is along the 2-fold crystallographic axis that lies between the two symmetry-related copies of Ser 72.

Table 7. Intermolecular Contacts Involving the Flap (Ser72−Ser82)

residue	residue of adjacent molecules	no. of contacts (<4.0 Å)	
		1	Cryo_**1**[a]
Ser72	Ser72		7(1)[b]
	Ile73		1
	Ser74	2	1
Ile73	Ser72		1
Ser74	Gly68		1
	Thr70		12(2)
	Trp71		3
	Ser72	2	1
	Glu133	1	
Gly76	Gly205		4
	Asp206		3
Asp77	Ser204		2
	Gly205		1
	Asp206		6
Gly78	Ser204		2

[a] Cryo_**1** = **1** at 110 K. [b] Numbers in parentheses indicate the possible hydrogen-bonding interactions included in the values given.

penicillopepsin is surprising (Table 5). Furthermore, the phosphonyl group is not located in the position within hydrogen-bonding distance of the two catalytic residues Asp33 and Asp213, as are the phosphonyl groups in the other phosphorus-containing inhibitors. The distance between the phosphorus atoms in the bound conformations of **3** and **1** is 3.19 Å (Figure 9).

Figure 10 presents the very distinctive binding interactions between penicillopepsin and **3**. The striking feature is that a solvent molecule, W103, was found in the catalytic site of penicillopepsin, keeping the same nonbonded contacts with Asp33 and Asp213, as has the corresponding solvent molecule O39 in the native penicillopepsin.[42] The *pro-R* oxygen of the phosphonyl group forms a hydrogen bond to water W103, instead of displacing it. The distance from Asp33 Oδ2 to Asp213 Oδ1 is 2.92 Å, longer than that observed in the native penicillopepsin molecule (2.8 Å); shorter than the average distance (~3.0 Å) seen in other complexes with phosphonate-containing inhibitors.[10] There are several ordered solvent molecules in the active site region, involved in the binding interactions of the **3** complex. Water W25 forms a hydrogen-bonded bridge connecting what would be the carbonyl oxygen atom at P1 with Asp33 Oδ1 and water. Asp77 Oδ2 accepts one hydrogen bond from the amide NH at P1 and another from solvent molecule W277. Water W277 serves as a hydrogen bond bridge between solvent molecules W25 and Ser79 Oγ. The *pro-S* oxygen atom of the phosphonyl group is close to Asp77 and it accepts one hydrogen bond from Asp77 NH. The *pro-S* oxygen to Asp77 Oδ2 distance is 3.25 Å, just a normal van der Waals contact distance.

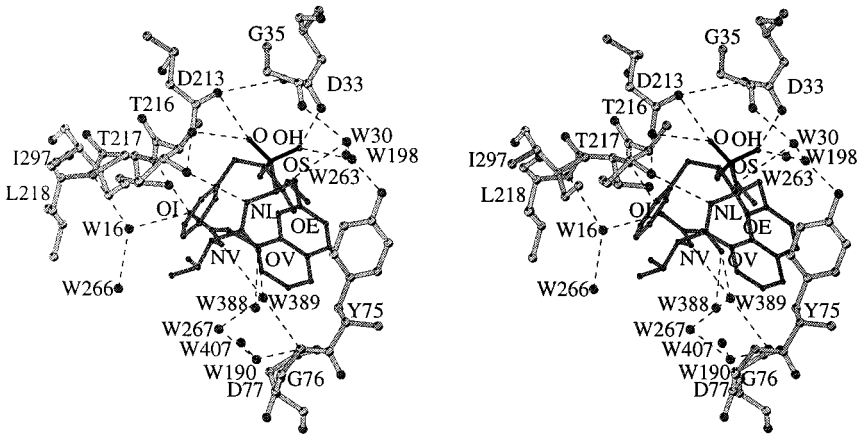

Figure 6. Stereoview of the hydrogen bonding with Cryo_**1** in the active site. The inhibitor is presented in black sticks; the enzyme is in gray sticks. Hydrogen bonds are shown as dashed lines.

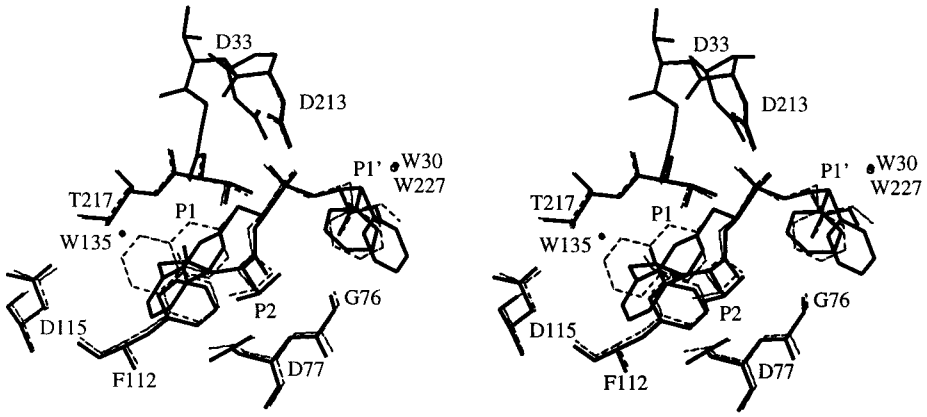

Figure 7. Superposition of penicillopepsin complexed with **1** and penicillopepsin complexed with **2**. **1** and residues in the active site are represented by solid lines, and the solvent molecules of this complex are represented by filled circles. The equivalent penicillopepsin residues and **2** are represented by dashed lines; the solvent molecule is by an open circle.

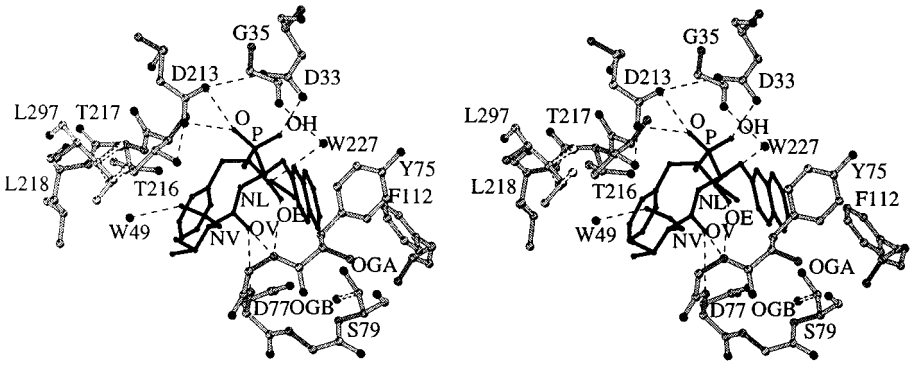

Figure 8. Stereoview of the hydrogen bonding with **2** in the active site. The inhibitor is presented in black sticks; the enzyme is in gray sticks. Hydrogen bonds are shown as dashed lines.

The main chain of the P1′ residue is stabilized by two hydrogen bonds. The hydrogen bond from Gly76 NH to the carbonyl oxygen atom of P1′ is also found in complexes with **1** and with **2**. Oxygen OP (equivalent to P1′ NH) accepts a proton from solvent molecule W324. A water channel is formed by water molecules W324, W276, W65, W228, W148, and W18. Water molecules W65, W148, and W18 are fixed by forming hydrogen bonds with penicillopepsin. This water channel is the hydrophilic environment in which the naphthyl ring at P3 is found. The main chain nitrogen atom of the P2 residue forms a hydrogen bond with Thr217 Oγ1. The carbonyl oxygen atom of P2 accepts two protons, one from Thr217 NH and the other from solvent molecule W50. Water W50 is within hydrogen-bonding distance of two main chain amide nitrogen atoms, Thr217 NH and Leu218 NH. Two other solvent molecules, W294 and W312, help to stabilize the N-terminus of **3** by forming two hydrogen bonds with the carbonyl oxygen atom at P3. W312 forms a hydrogen-bond bridge between OI and water W157.

Comparison of the Complex with 3 and the Complex with 4. As mentioned above, the acyclic, linear inhibitor **3** possesses unusual binding to penicillopepsin, since the phosphonyl group does not occupy the active site as a transition-state mimic. When superposing the main-chain atoms of the penicillopepsin structures in the **3** complex and in the **4** complex and transforming the inhibitor to that reference frame, we found it surprising that

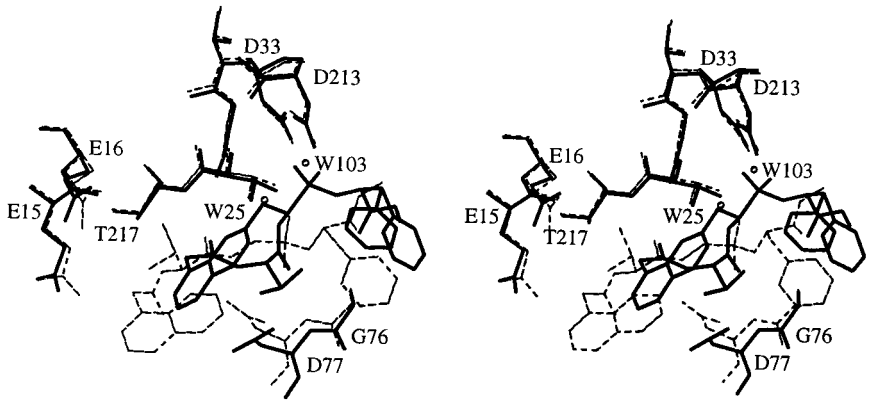

Figure 9. Superposition of penicillopepsin complexed with **1** and penicillopepsin complexed with **3**. **1** and residues in the active site are represented by solid lines. The equivalent penicillopepsin residues and **3** are represented by dashed lines, the solvent molecules are represented by open circles.

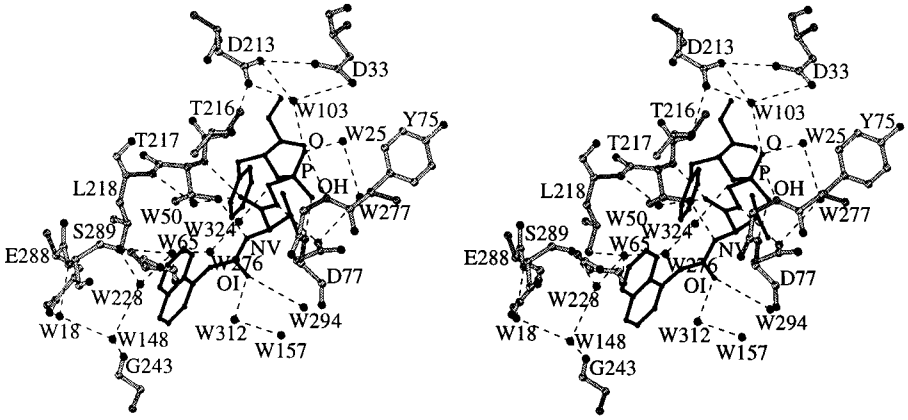

Figure 10. Stereoview of the hydrogen bonding with **3** in the active site. The inhibitor is presented in black sticks; the enzyme is in gray sticks. Hydrogen bonds are shown as dashed lines. Solvent molecules are represented by filled circles.

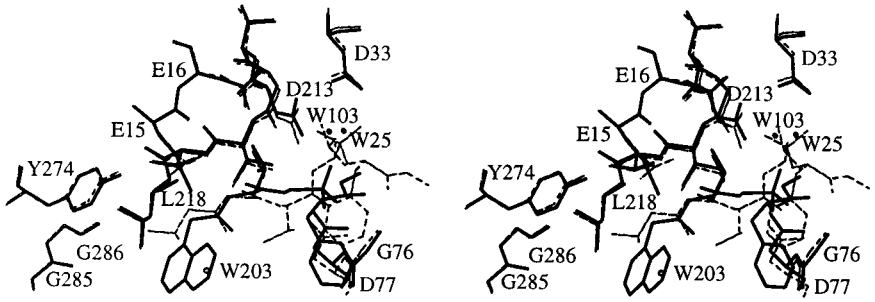

Figure 11. Superposition of penicillopepsin complexed with **3** and penicillopepsin complexed with **4**. **3** and residues in the active site are represented by solid lines, and the solvent molecules of this complex are represented by filled circles. The equivalent penicillopepsin residues and **4** in that complex are represented by dashed lines; the solvent molecules are represented by open circles.

the backbone of P3 to P1 of **3** adopted a similar conformation to that of P4 to P2 in **4**, and the P3 naphthalene group of **3** entered into the S4 pocket, kicking out water W203 found in the **4** complex (Figure 11). The presence of naphthalene in the S4 pocket does not bring about any large conformational changes in that region, since only individual residues adopt different side-chain conformations and several solvent molecules are redistributed. The rms displacement of 12 similar atoms (from P3 to P1 in **3**, without the phosphonyl group and naphthyl ring) is only 0.205 Å, showing the agreement with the corresponding part (from P4 to P2 in **4**, without the P2 and P4 side chains and P2 carbonyl group). The binding interactions of P3 to the S4 pocket in the **3** complex will contribute somehow to the inhibition constant, K_i. However, the K_i value of **3** is still relatively weak at 110 μM,[9] due to the fewer binding interactions between the penicillopepsin molecule and **3** because of the ~3.0 Å shift of the phosphonyl group away from the catalytic residues of penicillopepsin. It is very possible that the binding of the naphthalene group in the S4 pocket hindered **3** from contacting the catalytic residues of penicillopepsin. It is tempting to view this complex as an intermediate that got stuck along the pathway for binding, as if the presence of the naphthalene group in the S4 pocket blocked the rest of the molecule from settling into the thermodynamically favored, "peptidic" orientation in the active site. However, the inhibitor−enzyme complexes were formed in solution and it is likely that they reached their lowest energy orientations prior to crystallization.

Solvent-Accessible Surface. A major determinant of an inhibitor's binding affinity is the amount of hydrophobic surface—both on the enzyme as well as the inhibitor—that is sequestered from solvent on formation of the complex.[43−45] Pepsin is known to have a strong preference for hydrophobic

amino acids in oligopeptide substrates.[46] The two acyclic inhibitors have a little more hydrophobic surface area than the macrocyclic inhibitor as a result of replacing methylene units with hydrogens; if fully manifested on binding, this difference should favor the acyclic analogues by 0.5−1.0 kcal/mol.[9] The total amount of solvent-accessible surface area that is buried on binding is about 80% (Table 6), comparable to that of other acyclic penicillopepsin inhibitors.[10] [The relatively low percentage of buried surface area in Cryo_**1** in part results from the loss of interactions with the residues on the flap.]

Conclusions

As noted in the preceding paper, the macrocyclic design of **1** was successful in constraining the peptide backbone of the inhibitor to the conformation required for binding; indeed, the correspondence between the structure determined for **1** in solution and that found in the active site is remarkable. However, the orientation of the naphthalene unit in **1** does not appear to be optimal, since it prevents the flap over the enzyme active site from adopting the fully closed position seen in complexes with more conventional, acyclic inhibitors, and since the naphthyl side chain reorients significantly when the macrocyclic constraint is relaxed in **2**. It is not clear how much the unfavorable orientation of the naphthalene bridge in **1** costs in terms of binding energy, but it clearly acts to reduce the advantage conveyed by the macrocyclic constraint.

The binding orientation observed for the linear analogue **3** is surprising, since there is no apparent reason it cannot adopt a more conventional position in the active site. If the observed position is indeed its thermodynamic minimum, the dissociation constant for the orientation corresponding to that of the macrocycle would be even higher than the measured value of 110 μm and the difference in affinity as a result of the macrocyclic constraint in **1** even greater than 2 orders of magnitude. In conclusion, while it is apparent that the macrocyclic constraint of **1** enhances its binding affinity over the acyclic analogues, the subtle and not-so-subtle differences in their binding orientations mean that a quantitative demonstration of the effect has yet to be achieved.

Acknowledgment. We are indebted to Theo Hofmann for the supply of penicillopepsin. The work in Edmonton has been supported by a grant to the MRC Group in Protein Structure and Function and by grant MRC MT12831, both from the Medical Research Council of Canada. The work in Berkeley is supported by grant GM-30759 from the National Institutes of Health.

JA973714R

(43) Chothia, C. *Nature* **1974**, *248*, 338−339.
(44) Chothia, C. *J. Mol. Biol.* 1976, *105*, 1−14.
(45) Chothia, C.; Janin, J. *Nature* **1975** *256*, 705−708.
(46) Powers, J. C.; Harley, A. D.; Myers, D. V. In *Acid Proteases, Structure, Function and Biology*; Tang, J., Ed.; Plenum Press: New York, 1977; pp 141−157.